

The Structure, Anharmonic Vibrational Frequencies, and Intensities of NNHNN⁺

Qi Yu,[†] Joel M. Bowman,^{*,†} Ryan C. Fortenberry,^{*,‡} John S. Mancini,[†] Timothy J. Lee,[¶] T. Daniel Crawford,[§] William Klemperer,^{||} and Joseph S. Francisco[⊥]

*Department of Chemistry and Cherry L. Emerson Center for Scientific Computation,
Emory University, Atlanta, Georgia 30322, U.S.A., Georgia Southern University,
Department of Chemistry, Statesboro, GA 30460 U.S.A., NASA Ames Research Center,
Moffett Field, California 94035-1000, U.S.A., Department of Chemistry, Virginia Tech,
Blacksburg, Virginia 24061, U.S.A., Department of Chemistry, Harvard University,
Cambridge, Massachusetts 02138, U.S.A., and Department of Chemistry, University of
Nebraska-Lincoln, Lincoln, Nebraska 68588, U.S.A.*

E-mail: jmbowma@emory.edu; rfortenberry@georgiasouthern.edu

*To whom correspondence should be addressed

[†]Emory University

[‡]Georgia Southern University

[¶]NASA Ames Research Center

[§]Virginia Tech

^{||}Harvard University

[⊥]University of Nebraska-Lincoln

Abstract

A semi-global potential energy surface (PES) and quartic force field (QFF) based on fitting high-level electronic structure energies are presented to describe the structures and spectroscopic properties of NNHNN⁺. The equilibrium structure of NNHNN⁺ is linear with the proton equidistant between the two nitrogen groups and thus of $D_{\infty h}$ symmetry. Vibrational second-order perturbation theory (VPT2) calculations based on the QFF fails to describe the proton “rattle” motion, i.e., the antisymmetric proton stretch, due to the very flat nature of PES around the global minimum, but performs properly for other modes with sharper potential wells. Vibrational self-consistent field/virtual state configuration interaction (VSCF/VCI) calculations using a version of MULTIMODE without angular momentum terms successfully describe this motion and predict the fundamental to be at 759 cm⁻¹. This is in good agreement with the value of 746 cm⁻¹ from a fixed-node diffusion Monte Carlo calculation and the experimental Ar-tagged result of 743 cm⁻¹. Other VSCF/VCI energies are in good agreement with other experimentally reported ones. Both double-harmonic intensity and rigorous MULTIMODE intensity calculations show the proton transfer fundamental has a very strong intensity.

Keywords: Vibrational Configuration Interaction, Proton-Bound Complex, Molecular Lines, Astrochemistry

Introduction

N_2H^+ , known as diazenylium, is one of the first molecules observed in interstellar clouds. It was first observed in 1974 by B.E. Turner¹ with a triplet of microwave lines at 93.174 GHz confirming earlier suspicions of its interstellar presence.² The observations of N_2H^+ provide a rotational tracer of the nitrogen molecule in gas clouds where it should exist in observable abundance, but such is precluded by the lack of a dipole moment in N_2 . Both experimental and theoretical work have investigated the rotational and vibrational spectra of N_2H^+ in the last four decades. Based on its spectra, N_2H^+ is one of the most often observed interstellar molecules by astronomers. The ubiquity of N_2H^+ and N_2 in interstellar clouds leads to the reasonable assumption that there exists a novel and interesting, centrosymmetric molecular cation, $\text{NN-H}^+\text{-NN}$.

NNHNN^+ can result from gas phase reactions of N_2 and N_2H^+ similar to the production of OCHCO^+ .³ Both of these cations belong to the class of so called proton-bound complexes. In these complexes, the vibrational frequencies of the proton provide important information about the proton transfer process. Even though NNHNN^+ and OCHCO^+ are isoelectronic partners with one another, they present totally different properties for their vibrational frequencies.⁴⁻⁶ Nesbitt and co-workers performed anharmonic vibrational calculations for these two linear complexes using a two-dimensional (2-D) model consisting of the symmetric and antisymmetric proton-stretch modes. For OCHCO^+ , they successfully predicted fundamental symmetric and antisymmetric stretching transition energies as $\nu_{sym} = 298 \text{ cm}^{-1}$ and $\nu_{asym} = 386 \text{ cm}^{-1}$ with a dissociation energy of 4634 cm^{-1} in the CCSD(T)/CBS limit. In our recent work,⁴ the equilibrium structure of OCHCO^+ is $C_{\infty v}$, while there exists a saddle point $D_{\infty h}$ structure at 393.6 cm^{-1} above the minimum creating a 2-D barrier and a degenerate double well. A semi-global, full-dimensional potential energy surface (PES) was used in two sets of full-dimensional vibrational calculations to determine the proton transfer fundamental to be roughly 300 cm^{-1} , which is roughly 86 cm^{-1} below the prediction from the 2-D model. One set of calculations was a fixed-node diffusion Monte Carlo (DMC) cal-

ulation and the second employed vibrational self-consistent field/virtual state configuration interaction calculations (VSCF/VCI)⁷⁻¹⁰ with the code MULTIMODE (MM).^{11,12} The latter calculations did not fully employ the correct Watson Hamiltonian for linear molecules. The error in neglecting the vibrational angular momentum terms was roughly 10 cm⁻¹ for the zero-point energy, compared to the rigorous DMC result.

For NNHNN⁺, both experiments^{6,13} and *ab initio* calculations^{5,6,14,15} have investigated this interesting linear molecular cation. The 2-D *ab initio* calculations show there is a very flat potential around the $D_{\infty h}$ global minimum structure and Terrill and Nesbitt predict the proton transfer fundamental frequency to be 849 cm⁻¹. However, Ar-tagged experiments by Duncan and co-workers report this proton antisymmetric stretch at 743 cm⁻¹. Thus, the 2-D result is high by roughly 100 cm⁻¹, which may result from the neglect of the other 8 vibrational modes or perhaps (though unlikely) from strong perturbations from the Ar atom. Thus, more advanced anharmonic computational treatments need to investigate the vibrational frequencies and relevant spectroscopic properties of this cation.

There are two widely-used, general methods that consider anharmonicity in vibrational calculations. One is vibrational second order perturbation theory (VPT2)¹⁶⁻¹⁸ uses quadratic, all relevant cubic, and quartic force constants to create a quartic force field (QFF) utilized to calculate vibrational frequencies of polyatomic molecules, and this approach is based directly upon *ab initio* electronic structure data. Another method is configuration interaction calculations, analogous to those done in electronic structure theory and are applied here. Specifically, these start with a vibrational self-consistent field (VSCF) calculation of a reference state and then the associated virtual states are used in the subsequent CI calculations. This approach, denoted VSCF/VCI is, again, implemented in the code MM. Both of these methods are applied here to the study of the N₂ and N₂H⁺ proton-bound complex. A third method that is less widely used, the aforementioned diffusion Monte Carlo (DMC) method,^{19,20} is also used here to rigorously determine the zero-point energy and also the antisymmetric stretch proton fundamental, using an assumed fixed-node location for that

excited state.

This paper is organized as follows. In the next section, we present computational details of *ab initio* electronic structure calculations, the QFF construction, and the PES fitting procedure together with a dipole moment surface (DMS) fitting. Details of the various vibrational calculations are then given. Results of vibrational calculations and relevant properties of the PES are reported afterwards, along with comparisons with available experimental data. This work wraps up with a statement of the summary and conclusions.

Computational Details

QFF construction

The (QFF), a fourth-order Taylor series expansion of the internuclear potential operator, is generated for NNHNN⁺ in a similar fashion for this molecule as it has been done with other systems producing high-accuracy.²¹⁻²⁹ The geometry is optimized with MOLPRO 2010.1³⁰ the coupled cluster singles, doubles, and perturbative triples [CCSD(T)] method³¹ with the aug-cc-pV5Z basis set.³² Corrections for differences in CCSD(T) optimized geometries for inclusion and neglect of core orbitals through the Martin-Taylor (MT) core-correlating basis set³³ are added to the CCSD(T)/aug-cc-pV5Z structure to produce the reference geometry. From this geometry, a grid of 1181 points with displacements of 0.005 Å or 0.005 rad,

depending upon the mode, are produced through the following coordinates:

$$S_1(\Sigma_g^+) = (N_1 - N_2) + (N_3 - N_4) \quad (1)$$

$$S_2(\Sigma_g^+) = (N_2 - H) + (N_3 - H) \quad (2)$$

$$S_3(\Sigma_u^+) = (N_1 - N_2) - (N_3 - N_4) \quad (3)$$

$$S_4(\Sigma_u^+) = (N_2 - H) - (N_3 - H) \quad (4)$$

$$S_5(\Pi_g[xz]) = (\angle N_1 - N_2 - H - \mathbf{y}) + (N_3 - N_4 - H - \mathbf{y}) \quad (5)$$

$$S_6(\Pi_g[xz]) = (\angle N_2 - H - N_3 - \mathbf{y}) \quad (6)$$

$$S_7(\Pi_g[yz]) = (\angle N_1 - N_2 - H - \mathbf{x}) + (N_3 - N_4 - H - \mathbf{x}) \quad (7)$$

$$S_8(\Pi_g[yz]) = (\angle N_2 - H - N_3 - \mathbf{x}) \quad (8)$$

$$S_9(\Pi_u[xz]) = (\angle N_1 - N_2 - H - \mathbf{y}) - (N_3 - N_4 - H - \mathbf{y}) \quad (9)$$

$$S_X(\Pi_u[yz]) = (\angle N_1 - N_2 - H - \mathbf{x}) - (N_3 - N_4 - H - \mathbf{x}) \quad (10)$$

At each displaced geometry, a three-point³⁴ complete basis set (CBS) energy is produced from aug-cc-pVTZ, aug-cc-pVQZ, and aug-cc-pV5Z CCSD(T) energies. An energy correction for core correlation again with the MT basis set is also added to the energy. A final correction for scalar relativity³⁵ further completes the energy description utilized. This so-called CcCR QFF named for CBS (“C”), core correlation (“cC”), and relativity (“R”) corrections is then fit via a least squares method to produce the equilibrium geometry and zero gradients. The refit of the surface with the new minimum gives the force constants that are then transformed into Cartesian coordinates through the INTDER³⁶ program. Second-order perturbation theory for vibrations (VPT2)^{17,18} and rotations³⁷ is then utilized through SPECTRO³⁸ to produce the anharmonic vibrational frequencies and spectroscopic constants. Inclusion of resonances further enhances the VPT2 computations. Type-1 Fermi resonances include $2\nu_5 = 2\nu_6 = \nu_3$ & $2\nu_4 = \nu_1$, and Darling-Denison resonances include and ν_2/ν_1 , ν_7/ν_6 , and ν_6/ν_5 .

PES and DMS fitting details

A semi-global (PES) and corresponding (DMS) are constructed for use in the DMC and VSCF/VCI computations. This PES is a fit to 11,892 electronic energies calculated by the CCSD(T)-F12b method³⁹ with properly modified aug-cc-pVTZ basis set,⁴⁰ while the DMS uses Møller-Plesset second-order perturbation theory (MP2)⁴¹ method with aug-cc-pVTZ set for the same data configurations. The fitting procedure chosen uses a basis of permutationally invariant polynomials in Morse variables.⁴² Thus, the expression for the PES is as follows:

$$V(y) = \sum_{n=0}^6 h_n[p(y)]q_n(y) \quad (11)$$

where h_n is a polynomial of $p(y)$, a set of primary invariant polynomials, $q_n(y)$ are secondary invariant polynomials, and y is a set of Morse-like variables y_i . Each y_i is a Morse-type function of the form $y_{ij} = \exp(-r_{ij}/\alpha)$. The α value is fixed at 2.0 bohr, and r_{ij} is the distance between two atoms i and j .

The polynomial order for the PES is 6 with 495 linear coefficients for standard linear least-squares fitting. The total root mean square (RMS) fitting error is 0.6 cm^{-1} . As to the DMS, the fitting order we use is 5 with 844 total coefficients. The final RMS is 2×10^{-4} Debye.

Details of diffusion Monte Carlo and MM vibrational calculations

The PES and DMS are utilized in the DMC and MM calculations. In addition, a simple 1-D calculation, using a relaxed potential⁴³ in the proton antisymmetric stretch is also reported with the eigenstates obtained numerically. The DMC method provides essentially exact results for the zero-point energy as well as the wave function using the full-dimensional PES. Furthermore, fix-node DMC calculations provide accurate results for excited states, if the nodal surface can be accurately determined, e.g., by symmetry. The proton transfer fundamental is one example of such a state. In the DMC calculations, 3 independent trajectories

were performed with 40,000 steps and 40,000 initial walkers. For the excited state, the node is placed equidistant between the two flanking nitrogen atoms.

MM approaches vibrational calculations differently. It is important to note that the present code does not exactly described the kinetic energy terms for a linear molecule. As a result, vibrational angular momentum terms are not included when running MM. MM uses a n -mode representation (nMR) of the potential energy⁹ given by

$$V(Q_1, Q_2, Q_3, \dots, Q_N) = \sum_{i=1}^N V^{(1)}(Q_i) + \sum_{i>j}^N V^{(2)}(Q_i, Q_j) + \sum_{i>j>k}^N V^{(3)}(Q_i, Q_j, Q_k), \dots, \quad (12)$$

where, for example, summations are truncated at $V^{(3)}(Q_i, Q_j, Q_k)$ give a 3MR of V . In general, the nMR must be of at least order $n = 3$. For NNHNN⁺, n ranges from 4 to 6. Note $n = 10$ is an exact representation of V for this system; however, the matrix elements over V would require 10-dimensional numerical quadratures, as compared to 4-6 dimensional quadratures in the present case. The Watson Hamiltonian (without the vibrational angular momentum terms) is set up and then diagonalized to provide energies and eigenfunctions. In the present calculations, which are aimed at low-lying fundamental and combination states, the size of matrix is roughly of order 30,000 in the 5MR and 6MR calculations. Intensity calculations are carried out also using MM with CI wave functions from 5MR results, and these can be compared with the double-harmonic intensities obtained from the aforementioned MP2/aug-cc-pVTZ computations utilizing Gaussian09.^{41,44}

Results and Discussion

QFF results

The geometrical parameters from the CcCR QFF VPT2 results are given in Table 1. The short N≡N equilibrium bond and the longer N–H bond match that from previous computation.¹⁵ Both bonds shorten to 1.271 890 Å and 1.089 722Å, respectively, upon inclusion

of (R_α) vibrational averaging. The 2507.609 MHz CcCR equilibrium rotational constant is subsequently close to that previously determined, as well.¹⁵ Deuteration of the central proton increases the bond lengths slightly and also decreases B_0 by 2.332 MHz. The strong N \equiv N bond is mirrored in the 23.553 870 mdyn/ \AA^2 F_{11} force constant given in Table 2. This is in line¹⁴ with the N \equiv N bond in N₂H⁺ and even stronger than the N–N bond in NNOH⁺ where the force constant is determined in the latter²⁷ to be 21.257 633 mdyn/ \AA^2 . C \equiv C bonds are often less than 60% of this strength from our experience. The cubic force constants are also given in Table 2, while the quartic force constants are in Table 3.

The harmonic vibrational frequencies in Table 1 also closely mirror those from previous computation¹⁵ with one major exception, the ν_7 proton “rattle” motion which is 0.0 cm⁻¹ presently but is 159 cm⁻¹ in the previous results. This discrepancy is largely due to the very flat potential energy surface present for NNHNN⁺ with regards to the antisymmetric proton. Accurately predicting such behavior in this and related molecules is a known issue in computational spectroscopy.^{4,5,15} The global $D_{\infty h}$ minimum rests on a nearly-flat surface where a $C_{\infty v}$ minimum with a N₃–H bond of 1.305 Å can be optimized with very tight convergence criteria. However, the difference in energy between these two minima separated by 0.035 Å is 0.064 cm⁻¹ less than the value for the rotational constant. Consequently, more reliable methods such as DMC and MM should be utilized to describe ν_7 . However, while previous work on the related OCHCO⁺ cation⁴ showed that the QFF was insufficient for all but the two highest frequency modes, the CcCR QFF VPT2 results should be valid for all but this delocalized mode. This is discussed below with comparison between the QFF VPT2 results and those from DMC and MM.

In any case, the anharmonic frequencies behave as expected, again, save for ν_7 . Positive anharmonicities are present for all of the π modes, but non-totally symmetric modes are known to behave as such in linear or pseudo-linear molecules since the cubic force constants are typically quite small for these modes.^{25–27,45} Furthermore, there is little shift between the harmonic and even anharmonic frequencies in NNHNN⁺ and those in NNDNN⁺ as a

result of the proton or deuteron residing at the center-of-mass except for the obvious ν_4 out-of-plane proton motion with some shift also produced in the ν_6 antisymmetric bending mode. The MP2/aug-cc-pVTZ double harmonic intensities^{41,44} of NNHNN⁺ are relatively proportionate to the same values for the same modes in OCHCO⁺. The NNHNN⁺ proton-rattle mode is again the brightest at 5170 km/mol, which is actually within 1% of that from OCHCO⁺. Additionally, the vibrationally-excited rotational constants are also provided in Table 1 since some of these can be observed experimentally. Unfortunately, the reported B_7 value for this bright mode is not trustworthy. It has a 0.0 vibration-rotation interaction constant as a result of the VPT2 anharmonic frequency being nearly 0 cm⁻¹ making it the same as B_0 .

PES properties

The fidelity of the PES is determined in three important ways, shown in Tables 4 and 5. In the first, the equilibrium geometry is reported from both the PES and directly from *ab initio* calculations. As seen, agreement between the two approaches is excellent. The absolute electronic energy is also accurately reproduced by the PES. Additionally, the harmonic frequencies from the PES are in very good agreement with those from *ab initio* calculations, the only exception being the out-of-plane proton bend. Further good agreement is also present for the harmonic frequencies from the QFF shown in Table 1 and these other methods. That being said, there are some ~ 15 cm⁻¹ differences between the QFF and PES harmonic frequencies, but these are almost certainly the result of the proton being delocalized. Finally, the DMC calculations, which sample large regions of the PES away from the global minimum indicate that the PES has no regions of unphysical behavior that are sampled by the DMC walkers. (DMC calculations were used to add configurations to the initial database of configurations in order to eliminate problematic regions that were sampled by DMC walkers.) The PES does not describe dissociation and so it would produce unphysical results in that region.

In Fig. 1 the relaxed 1-D potential as a function of the proton transfer normal mode is

shown. The numerically computed first two eigenvalues are indicated. As seen, the potential is highly anharmonic. The PES is quite flat around the equilibrium and then rises very steeply creating the deep well previously determined.¹⁵ Fig. 2 shows the DMC energies for the ground and first excited proton transfer states as function of the imaginary time variable for one trajectory utilizing 40,000 walkers. The associated wavefunctions are shown in isosurface plots in Figs. Fig. 3 and Fig. 4. These figures highlight the delocalized behavior about the central proton in NNHNN⁺.

Comparisons among theoretical results and to experiment

In comparing the QFF with VPT2 to the other approaches utilized in this work, it is clear that the delocalized proton “rattle” motion in NNHNN⁺ cannot be robustly computed within the present methodology. However, larger step-sizes may rectify this issue since the potential is so deep. Such an exercise is left for later analysis. Furthermore, the \perp proton motion is also ineffectively described with the CcCR QFF and VPT2.

However, as shown in Table 6, many other modes are well-described by the QFF compared to MM. It should be noted that computation of the CcCR QFF required substantially more computational time than the more numerous, but less costly individual CCSD(T)-F12b/aug-cc-pVTZ points used to define the MM PES. Conversely, the VPT2 computations themselves are less costly than the MM results. Hence, a trade-off is present in terms of time and accuracy. The ν_2 , ν_5 , and ν_6 QFF VPT2 and 5 and 6MR MM frequencies are all within 9 cm^{-1} of one another with the two lower frequency modes within about 3 cm^{-1} . Since both approaches solve the anharmonic vibrational Schrödinger equation differently and are based on different PES constructions, it implies that these modes are properly described by both approaches. The DMC result for the ν_1 proton transfer fundamental agrees well with the approximate 5MR MM result, and agreement with experiment is also very good. Finally, it is notable that the result of the 1-D calculation for this fundamental is significantly higher than the MM and DMC results, indicating the importance of coupling to the other vibrational

modes.

The solid consistency between the VPT2 and MM results, except for ν_7 , is corroborated for both approaches by the generally good comparison to experiment also given in Table 6. Note that four experimental numbers are derived from putative assignments of combination bands and the assumption of simple additivity of fundamentals. The ν_1 and ν_4 frequencies are not as consistent numerically between the two approaches, but they do not vary by more than 20 cm^{-1} . In fact, the 5MR results find this band to be highly mixed, and, thus, two candidate energies are given in the table. The “derived” experimental value for this band deviates the most from theory. As a result, it is shown here that highly-accurate QFFs with even VPT2 can mirror highly-descriptive MM results for modes with localized vibrational wave functions. Delocalized motions like the proton “rattle” in both NNHNN^+ and OCHCO^+ are not properly described with QFFs and VPT2, as has also been observed for the heavy atom frequencies of noble gas complexes.⁴⁶ Such modes likely require high-level VSCF/VCI or DMC computations for even at least qualitative accuracy, much less near-spectroscopic accuracy.

Additionally, the DMS and double-harmonic intensities corroborate very well, especially from a qualitative perspective. MP2 intensities have been shown to perform similarly to CCSD(T) values,⁴⁷ and such is supported here, again. The ν_2 , ν_4 , and ν_6 modes give closely related quantitative results, but the DMS ν_7 intensity is 57% that of the MP2. Even so, there is no mistaking that both produce incredibly bright intensities for the proton “rattle” motion. Quantitatively correct results should utilize a DMS approach, but MP2 intensities can provide a good first approximation.

Summary and conclusions

Ab initio quartic force fields and semi-global permutationally invariant potential energy and dipole moment surfaces were reported for NNHNN^+ and NNDNN^+ . These were used,

respectively, in VPT2 and VSCF/VCI calculations of low-lying vibrational states of NHNN^+ . Benchmark diffusion Monte Carlo calculations of the zero-point energy and proton-transfer fundamental were also reported, as were simple 1-D calculations using a relaxed potential in that mode. While the MM results are absolutely necessary to describe any delocalized nuclear motion, the more localized modes are effectively described by the CcCR QFF utilizing VPT2. Furthermore, spectroscopic properties are also provided by this method to encapsulate fully the rotational and rovibrational spectra of NNHNN^+ . Finally, comparisons with results from an Ar-tagged predissociation experimental spectrum showed generally good agreement for bands that were measured explicitly or inferred from combination bands.

Beyond benchmarking the performance of these vibrational approaches, a full and accurate vibrational and rovibrational picture of this proton-bound cation complex is now provided. The exceptionally bright proton “rattle” motion will dominate the vibrational spectrum as shown in idealized form in Fig. 5. This terahertz feature should allow NNHNN^+ to be detected in interstellar environments even if its molecular concentrations are small. The NNHNN^+ cation complex may serve as a sink of interstellar N_2 with its 6139 cm^{-1} barrier to dissociation,¹⁵ and a ratio of NNHNN^+ to NNH^+ or N_2 in astrophysical regions like the protoplanetary disks surrounding the T Tauri star TW Hya and the Herbig Ae star HD 163296⁴⁸ will certainly enhance our understanding of the nitrogen budget of such regions.

Acknowledgements

The National Science Foundation grant No. CHE-1463552 supported the work done by JMB, QY, and JSM. RCF wishes to acknowledge Georgia Southern University for providing start-up funds utilized in this work. TDC acknowledges support from the U.S. National Science Foundation (NSF) through award CHE-1058420 and by NSF Multi-User Chemistry Research Instrumentation and Facility (CRIF:MU) award CHE-0741927 which provided the computer hardware employed. This work is also supported by the National Aeronautics and Space

Administration through the NASA Astrobiology Institute under Cooperative Agreement Notice NNH13ZDA017C issued through the Science Mission Directorate.

References

- (1) Turner, B. E. U93.174 - A New Interstellar Line with Quadrupole Hyperfine Splitting. *Astrophys. J.* **1974**, *193*, L83–L84.
- (2) Green, S.; Montgomery, J. A.; Thaddeus, P. Tentative identification of U93.174 as the molecular ion N_2H^+ . *Astrophys. J.* **1974**, *193*, L89–L91.
- (3) Jennings, K. R.; Headley, J. V.; Mason, R. S. The temperature dependence of ion-molecule association reactions. *Int. J. Mass. Spectrom. Ion Phys.* **1982**, *45*, 315–322.
- (4) Fortenberry, R. C.; Yu, Q.; Mancini, J. S.; Bowman, J. M.; Lee, T. J.; Crawford, T. D.; Klemperer, W. F.; Francisco, J. S. Spectroscopic Consequences of Proton Delocalization in OCHCO^+ . *J. Chem. Phys.* **2015**, *143*, 071102.
- (5) Terrill, K.; Nesbitt, D. J. *Ab initio* anharmonic vibrational frequency predictions for linear proton-bound complexes $\text{OC}-\text{H}^+-\text{CO}$ and $\text{N}_2-\text{H}^+\text{N}_2$. *Phys. Chem. Chem. Phys.* **2010**, *12*, 8311–8322.
- (6) Verdes, D.; Linnartz, H.; Maier, J. P.; Botschwina, P.; Oswald, R.; Rosmus, P.; Knowles, P. J. Spectroscopic and theoretical characterization of linear centrosymmetric $\text{N}\equiv\text{N}\cdots\text{H}^+\cdots\text{N}\equiv\text{N}$. *J. Chem. Phys.* **1999**, *111*, 8400.
- (7) Bowman, J. M. Self-consistent field energies and wavefunctions for coupled oscillators. *J. Chem. Phys.* **1978**, *68*, 608.
- (8) Bowman, J. M. The self-consistent-field approach to polyatomic vibrations. *Acc. Chem. Res.* **1986**, *19*, 202–208.

- (9) Carter, S.; Culik, J. S.; Bowman, J. M. Vibrational self-consistent field method for many-mode systems: A new approach and application to the vibrations of CO adsorbed on Cu(100). *J. Chem. Phys.* **1997**, *107*, 10458.
- (10) Christoffel, K. M.; Bowman, J. M. Investigations of self-consistent field, scf ci and virtual stateconfiguration interaction vibrational energies for a model three-mode system. *Chem. Phys. Lett.* **1982**, *85*, 220–224.
- (11) Bowman, J. M.; Carter, S.; Huang, X. MULTIMODE: A code to calculate rovibrational energies of polyatomic molecules. *Int. Rev. Phys. Chem.* **2003**, *22*, 533.
- (12) Bowman, J. M.; Carrington, T.; Meyer, H.-D. Variational quantum approaches for computing vibrational energies of polyatomic molecules. *Mol. Phys.* **2008**, *106*, 2145.
- (13) Ricks, A. M.; Douberly, G. E.; Duncan, M. A. Infrared spectroscopy of the protonated nitrogen dimer: The complexity of shared proton vibrations. *J. Chem. Phys.* **2009**, *131*, 104312.
- (14) Huang, X.; Valeev, E. F.; Lee, T. J. Comparison of one-particle basis set extrapolation to explicitly correlated methods for the calculation of accurate quartic force fields, vibrational frequencies, and spectroscopic constants: Application to H₂O, N₂H⁺, NO₂⁺, and C₂H₂. *J. Chem. Phys.* **2010**, *133*, 244108.
- (15) Mladenovčić, M.; Roueff, E. Ion-Molecule Reactions involving HCO⁺ and N₂H⁺⁺ Isotopologue Equilibria from New Theoretical Calculations and Consequences for Interstellar Isotope Fractionation. *Astron. Astrophys.* **2014**, *566*, A144.
- (16) Nielsen, H. H. The Vibration-Rotation Energies of Molecules. *Rev. Mod. Phys.* **1951**, *23*, 90–136.
- (17) Mills, I. M. In *Molecular Spectroscopy - Modern Research*; Rao, K. N., Mathews, C. W., Eds.; Academic Press: New York, 1972; pp 115–140.

- (18) Watson, J. K. G. In *Vibrational Spectra and Structure*; During, J. R., Ed.; Elsevier: Amsterdam, 1977; pp 1–89.
- (19) Kosztin, I.; Faber, B.; Schulten, K. Introduction to the diffusion Monte Carlo method. *Am. J. Phys.* **1996**, *64*, 633.
- (20) McCoy, A. B. Diffusion Monte Carlo approaches for investigating the structure and vibrational spectra of fluxional systems. *Int. Rev. Phys. Chem.* **2006**, *25*, 77–107.
- (21) Huang, X.; Lee, T. J. A Procedure for Computing Accurate *Ab Initio* Quartic Force Fields: Application to HO_2^+ and H_2O . *J. Chem. Phys.* **2008**, *129*, 044312.
- (22) Huang, X.; Lee, T. J. Accurate *Ab Initio* Quartic Force Fields for NH_2^- and CCH and Rovibrational Spectroscopic Constants for Their Isotopologs. *J. Chem. Phys.* **2009**, *131*, 104301.
- (23) Huang, X.; Taylor, P. R.; Lee, T. J. Highly Accurate Quartic Force Field, Vibrational Frequencies, and Spectroscopic Constants for Cyclic and Linear C_3H_3^+ . *J. Phys. Chem. A* **2011**, *115*, 5005–5016.
- (24) Fortenberry, R. C.; Huang, X.; Francisco, J. S.; Crawford, T. D.; Lee, T. J. The *trans*-HOCO radical: fundamental vibrational frequencies, quartic force fields, and spectroscopic constants. *J. Chem. Phys.* **2011**, *135*, 134301.
- (25) Fortenberry, R. C.; Huang, X.; Francisco, J. S.; Crawford, T. D.; Lee, T. J. Quartic Force Field Predictions of the Fundamental Vibrational Frequencies and Spectroscopic Constants of the Cations HOCO^+ and DOCO^+ . *J. Chem. Phys.* **2012**, *136*, 234309.
- (26) Fortenberry, R. C.; Huang, X.; Francisco, J. S.; Crawford, T. D.; Lee, T. J. Fundamental Vibrational Frequencies and Spectroscopic Constants of HOCS^+ , HSCO^+ , and Isotopologues via Quartic Force Fields. *J. Phys. Chem. A* **2012**, *116*, 9582–9590.

- (27) Huang, X.; Fortenberry, R. C.; Lee, T. J. Protonated Nitrous Oxide, NNOH^+ : Fundamental Vibrational Frequencies and Spectroscopic Constants from Quartic Force Fields. *J. Chem. Phys.* **2013**, *139*, 084313.
- (28) Zhao, D.; Doney, K. D.; Linnartz, H. Laboratory Gas-Phase Detection of the Cyclopropenyl Cation ($c\text{-C}_3\text{H}_3^+$). *Astrophys. J. Lett.* **2014**, *791*, L28.
- (29) Fortenberry, R. C.; Huang, X.; Crawford, T. D.; Lee, T. J. Quartic Force Field Rovibrational Analysis of Protonated Acetylene, C_2H_3^+ , and Its Isotopologues. *J. Phys. Chem. A* **2014**, *118*, 7034–7043.
- (30) Werner, H.-J.; Knowles, P. J.; Manby, F. R.; Schütz, M.; Celani, P.; Knizia, G.; Korona, T.; Lindh, R.; Mitrushenkov, A.; Rauhut, G.; Adler, T. B.; Amos, R. D.; Bernhardsson, A.; Berning, A.; Cooper, D. L.; Deegan, M. J. O.; Dobbyn, A. J.; Eckert, F.; Goll, E.; Hampel, C.; Hesselmann, A.; Hetzer, G.; Hrenar, T.; Jansen, G.; Köppl, C.; Liu, Y.; Lloyd, A. W.; Mata, R. A.; May, A. J.; McNicholas, S. J.; Meyer, W.; Mura, M. E.; Nicklass, A.; Palmieri, P.; Pflüger, K.; Pitzer, R.; Reiher, M.; Shiozaki, T.; Stoll, H.; Stone, A. J.; Tarroni, R.; Thorsteinsson, T.; Wang, M.; Wolf, A. MOLPRO, version 2010.1, a Package of *Ab Initio* Programs. 2010; see <http://www.molpro.net>.
- (31) Raghavachari, K.; Trucks, G. W.; Pople, J. A.; Head-Gordon, M. A Fifth-Order Perturbation Comparison of Electron Correlation Theories. *Chem. Phys. Lett.* **1989**, *157*, 479–483.
- (32) Dunning, T. H. Gaussian Basis Sets for Use in Correlated Molecular Calculations. I. The Atoms Boron through Neon and Hydrogen. *J. Chem. Phys.* **1989**, *90*, 1007–1023.
- (33) Martin, J. M. L.; Taylor, P. R. Basis Set Convergence for Geometry and Harmonic Frequencies. Are h Functions Enough? *Chem. Phys. Lett.* **1994**, *225*, 473–479.
- (34) Martin, J. M. L.; Lee, T. J. The Atomization Energy and Proton Affinity of NH_3 . An *Ab Initio* Calibration Study. *Chem. Phys. Lett.* **1996**, *258*, 136–143.

- (35) Douglas, M.; Kroll, N. Quantum Electrodynamical Corrections to the Fine Structure of Helium. *Ann. Phys.* **1974**, *82*, 89–155.
- (36) Allen, W. D.; coworkers, 2005; *INTDER* 2005 is a General Program Written by W. D. Allen and Coworkers, which Performs Vibrational Analysis and Higher-Order Non-Linear Transformations.
- (37) Papousek, D.; Aliev, M. R. *Molecular Vibration-Rotation Spectra*; Elsevier: Amsterdam, 1982.
- (38) Gaw, J. F.; Willets, A.; Green, W. H.; Handy, N. C. In *Advances in Molecular Vibrations and Collision Dynamics*; Bowman, J. M., Ratner, M. A., Eds.; JAI Press, Inc.: Greenwich, Connecticut, 1991; pp 170–185.
- (39) Knizia, G.; Adler, T. B.; Werner, H.-J. Simplified CCSD(T)-F12 Methods: Theory and Benchmarks. *J. Chem. Phys.* **2000**, *130*, 054104.
- (40) Peterson, K. A.; Adler, T. B.; Werner, H.-J. Systematically Convergent Basis Sets for Explicitly Correlated Wavefunctions: The Atoms H, He, B, C, N, O, F, Ne, and Al, Si, S, Ar. *J. Chem. Phys.* **2008**, *128*, 084102.
- (41) Møller, C.; Plesset, M. S. Note on an Approximation Treatment for Many-Electron Systems. *Phys. Rev.* **1934**, *46*, 618–622.
- (42) Braams, B. J.; Bowman, J. M. Permutationally Invariant Potential Energy Surfaces in High Dimensionality. *Int. Rev. Phys. Chem.* **2009**, *28*, 577–606.
- (43) Wang, Y.; Bowman, J. M. Mode-Specific Tunneling Using the QIM Path: Theory and an Application to Full-Dimensional Malonaldehyde. *J. Chem. Phys.* **2013**, *139*, 154303.
- (44) Frisch, M. J.; Trucks, G. W.; Schlegel, H. B.; Scuseria, G. E.; Robb, M. A.; Cheeseman, J. R.; Scalmani, G.; Barone, V.; Mennucci, B.; Petersson, G. A.; Nakatsuji, H.;

Caricato, M.; Li, X.; Hratchian, H. P.; Izmaylov, A. F.; Bloino, J.; Zheng, G.; Sonnenberg, J. L.; Hada, M.; Ehara, M.; Toyota, K.; Fukuda, R.; Hasegawa, J.; Ishida, M.; Nakajima, T.; Honda, Y.; Kitao, O.; Nakai, H.; Vreven, T.; Montgomery, J. A., Jr.; Peralta, J. E.; Ogliaro, F.; Bearpark, M.; Heyd, J. J.; Brothers, E.; Kudin, K. N.; Staroverov, V. N.; Kobayashi, R.; Normand, J.; Raghavachari, K.; Rendell, A.; Burant, J. C.; Iyengar, S. S.; Tomasi, J.; Cossi, M.; Rega, N.; Millam, J. M.; Klene, M.; Knox, J. E.; Cross, J. B.; Bakken, V.; Adamo, C.; Jaramillo, J.; Gomperts, R.; Stratmann, R. E.; Yazyev, O.; Austin, A. J.; Cammi, R.; Pomelli, C.; Ochterski, J. W.; Martin, R. L.; Morokuma, K.; Zakrzewski, V. G.; Voth, G. A.; Salvador, P.; Dannenberg, J. J.; Dapprich, S.; Daniels, A. D.; Farkas, O.; Foresman, J. B.; Ortiz, J. V.; Cioslowski, J.; Fox, D. J. Gaussian 09 Revision D.01. Gaussian Inc. Wallingford CT 2009.

- (45) Huang, X.; Fortenberry, R. C.; Lee, T. J. Spectroscopic Constants and Vibrational Frequencies for $l\text{-C}_3\text{H}^+$ and Isotopologues from Highly-Accurate Quartic Force Fields: The Detection of $l\text{-C}_3\text{H}^+$ in the Horsehead Nebula PDR Questioned. *Astrophys. J. Lett.* **2013**, *768*, 25.
- (46) Theis, R. A.; Fortenberry, R. C. The Trihydrogen Cation with Neon and Argon: Structural, Energetic, and Spectroscopic Data from Quartic Force Fields. *J. Phys. Chem. A* **2015**, *119*, 4915–4922.
- (47) Fortenberry, R. C.; Huang, X.; Schwenke, D. W.; Lee, T. J. Limited Rotational and Rovibrational Line Lists Computed with Highly Accurate Quartic Force Fields and *Ab Initio* Dipole Surfaces. *Spectrochim. Acta, Part A*. **2014**, *119*, 76–83.
- (48) Qi, C.; Öberg, K. I.; Wilner, D. J. H_2CO and N_2H^+ in Protoplanetary Disks: Evidence for a CO-Ice Regulated Chemistry. *Astrophys. J.* **2013**, *765*, 34.

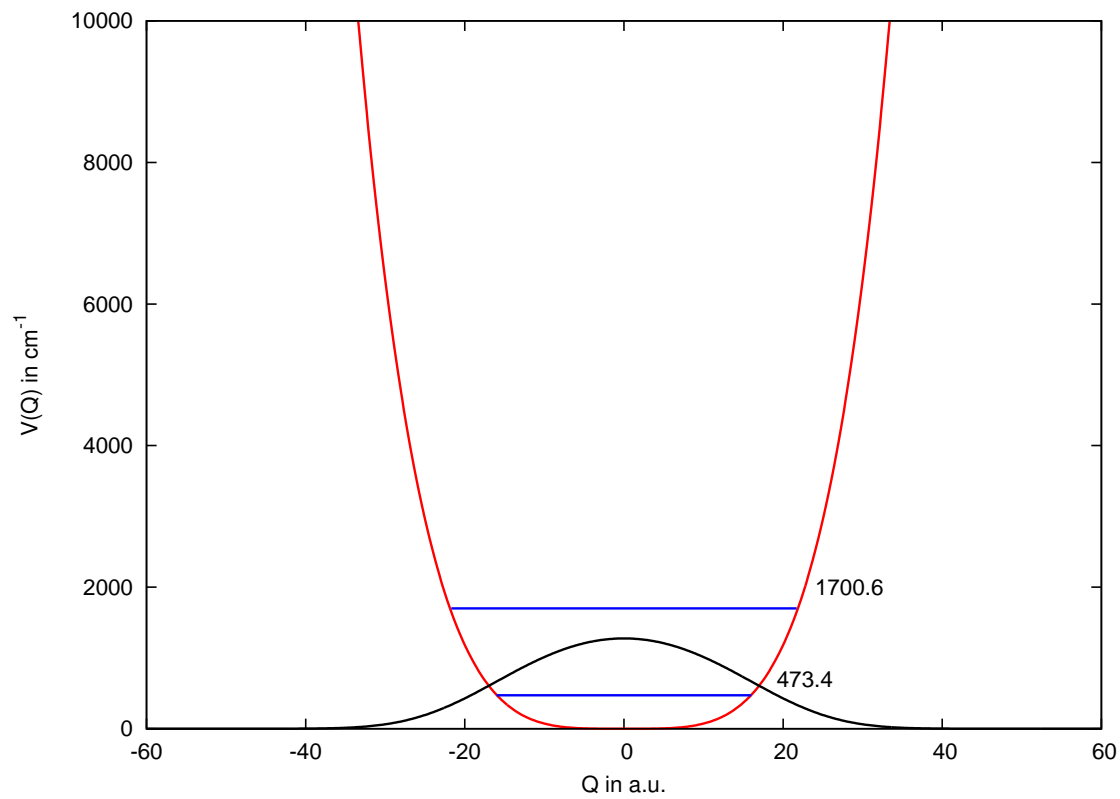


Figure 1: 1-D DVR calculation along proton transfer, ground state wavefunction and energies of ground and first excited states.

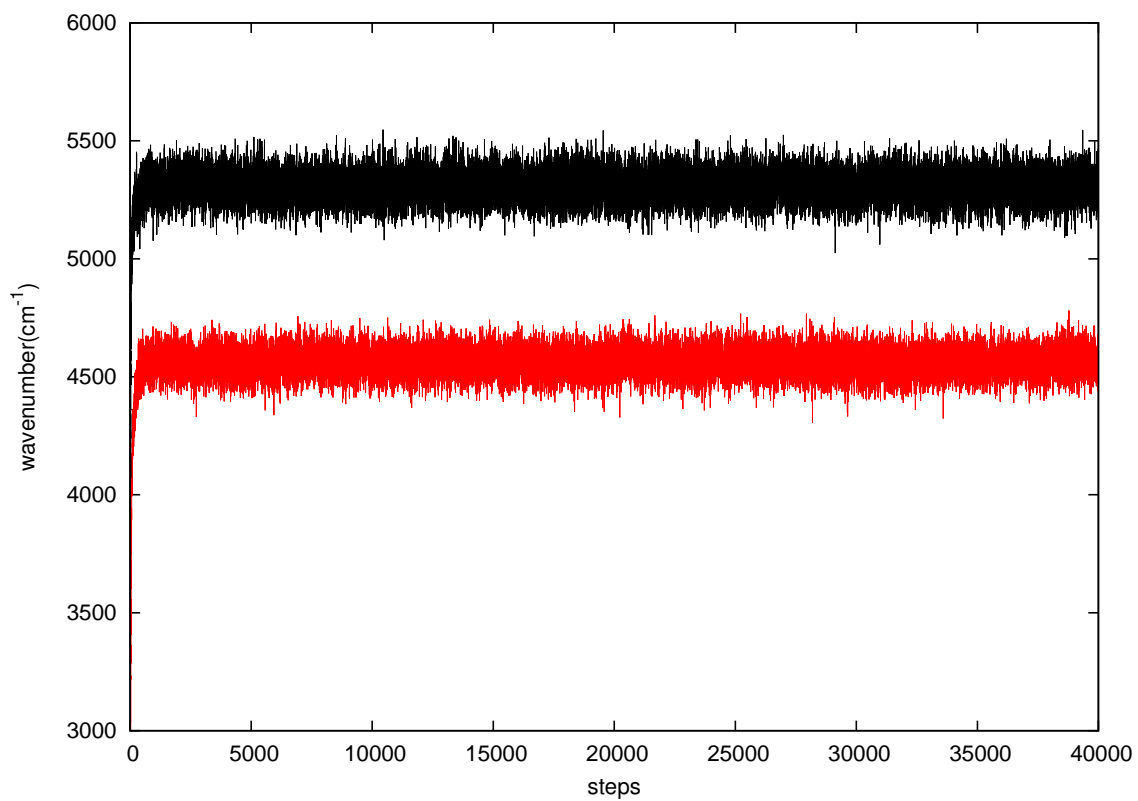


Figure 2: Trajectories of ground state and first excited state from diffusion Monte Carlo calculation



Figure 3: Diffusion Monte Carlo ground vibrational state wavefunction isosurface of NNHNN^+

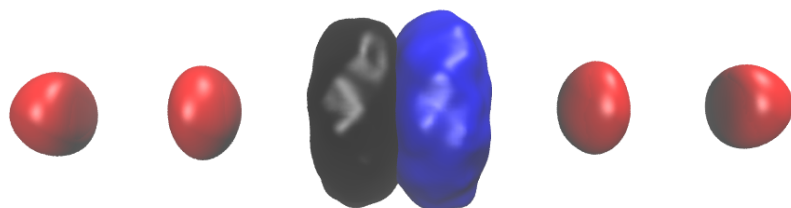


Figure 4: Diffusion Monte Carlo excited proton-transfer state wavefunction isosurface of NNHNN⁺

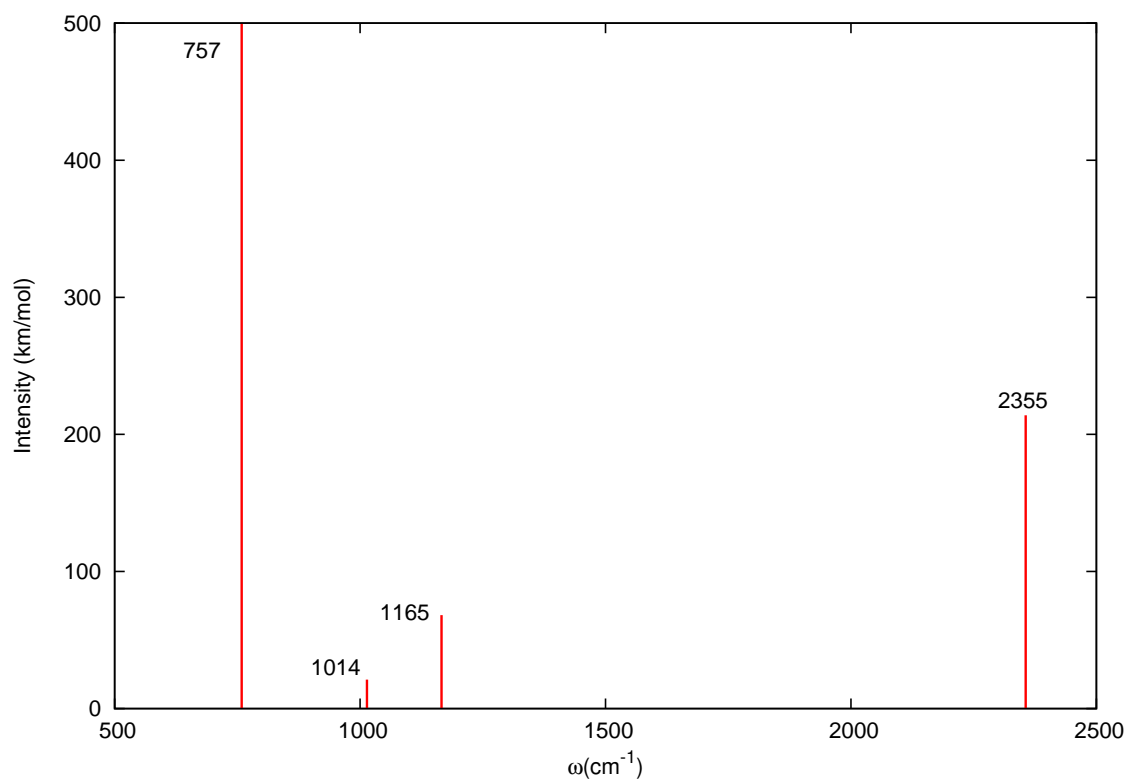


Figure 5: Intensities from MULTIMODE calculations

Table 1: The NNHNN⁺ and Deuterated Form Equilibrium and Zero-Point (R_α Vibrationally-Averaged) Minimum Structures, Vibrational Frequencies & Intensities^a, and Spectroscopic Data for the D_{∞h} CcCR QFF.

	NNHNN ⁺	NNDNN ⁺	Previous ^b
R ₀ (N–N)	1.089 722 Å	1.089 761 Å	–
R ₀ (N–H)	1.271 890 Å	1.272 803 Å	–
R _e (N–N)	1.096 769 Å	1.096 769 Å	1.101
R _e (N–H)	1.274 087 Å	1.274 087 Å	1.276
<i>B</i> ₀	2507.609	2505.277	–
<i>B</i> _e	2490.980	2490.980	2479
<i>D</i> _e	337.17 Hz	337.17 Hz	–
<i>H</i> _e	-137.38 Hz	-4.1949 Hz	–
α ^B 1	7.3 MHz	7.3 MHz	–
α ^B 2	6.7 MHz	6.5 MHz	–
α ^B 3	7.0 MHz	7.0 MHz	–
α ^B 4	-6.8 MHz	-4.6 MHz	–
α ^B 5	-8.0 MHz	-8.0 MHz	–
α ^B 6	-12.4 MHz	-12.2 MHz	–
α ^B 7	0.0 MHz	0.0 MHz	–
ω ₁ σ _g N–N symm. stretch	2433.4	2433.4	2402/2402
ω ₂ σ _u N–N antisymm. stretch	2397.8 (241)	2397.4	2365/2365
ω ₃ σ _g N–H symm. stretch	437.4	437.4	438/438
ω ₄ π _u ⊥ proton motion	1217.3 (86)	889.9	1235/902
ω ₅ π _g N–N–H symm. bend	263.8	263.9	265/265
ω ₆ π _u N–N–H antisymm. bend	138.5 (7)	135.2	144/140
ω ₇ σ _u N–H antisymm. stretch	0.0 (5170)	0.0	159/112
harmonic zero-point	4253.9	3923.1	4327/3967
ν ₁ σ _g N–N symm. stretch	2396.4	2400.3	–
ν ₂ σ _u N–N antisymm. stretch	2363.9	2364.7	–
ν ₃ σ _g N–H symm. stretch	432.5	432.3	–
ν ₄ π _u ⊥ proton motion	1302.3	936.5	–
ν ₅ π _g N–N–H symm. bend	278.2	275.4	–
ν ₆ π _u N–N–H antisymm. bend	148.7	139.8	–
ν ₇ σ _u N–H antisymm. stretch	0.6	0.5	–
zero-point	4299.4	3947.9	–
<i>B</i> ₁	2500.279	2497.947	–
<i>B</i> ₂	2500.924	2498.732	–
<i>B</i> ₃	2500.630	2498.297	–
<i>B</i> ₄	2514.363	2509.872	–
<i>B</i> ₅	2515.569	2513.236	–
<i>B</i> ₆	2520.023	2517.448	–
<i>B</i> ₇	2507.609	2505.277	–

^aMP2/aug-cc-pVTZ double harmonic intensities in parentheses for the vibrationally-active modes.

^bCCSD(T)/aug-cc-pVTZ geometrical parameters from Ref. 15. The deuterated harmonic frequencies fall on the right with the regular NNHNN⁺ on the left.

Table 2: The NNHNN⁺ CcCR QFF Quadratic and Cubic Force Constants^a (in mdyn/Åⁿ·rad^m).^b

F ₁₁	23.553 870	F ₂₂₁	-0.3913	F ₇₇₂	-0.0125
F ₂₁	-0.025 333	F ₂₂₂	-14.2105	F ₈₇₁	0.0495
F ₂₂	3.273 687	F ₃₃₁	-122.2284	F ₈₇₂	0.0951
F ₃₃	23.551 868	F ₃₃₂	-0.0310	F ₈₈₁	-0.0621
F ₄₃	-0.152 102	F ₄₃₁	0.2499	F ₈₈₂	-0.5596
F ₄₄	-0.003 333	F ₄₃₂	0.2943	F ₉₅₃	-0.2781
F ₅₅	0.163 160	F ₄₄₁	0.1981	F ₉₅₄	-0.1642
F ₆₅	-0.029 427	F ₄₄₂	-4.9153	F ₉₆₃	0.0522
F ₆₆	0.210 064	F ₅₅₁	-0.3035	F ₉₆₄	0.0336
F ₇₇	0.163 161	F ₅₅₂	-0.0125	F ₉₉₁	-0.2794
F ₈₈	0.210 064	F ₆₅₁	0.0495	F ₉₉₂	0.0108
F ₉₉	0.154 817	F ₆₅₂	0.0951	F _{X93}	0.0000
F _{XX}	0.154 817	F ₆₆₁	-0.0621	F _{X94}	-0.0001
F ₁₁₁	-122.3181	F ₆₆₂	-0.5596	F _{XX1}	-0.2794
F ₂₁₁	-0.0719	F ₇₇₁	-0.3035	F _{XX2}	0.0107

^aThe numbering is from the symmetry internal coordinates given in the Computational Details.

^b1 mdyn = 10⁻⁸ N; n and m are exponents corresponding to the number of units from the type of modes present in the specific force constant.

Table 3: The complete NNHNN⁺ CcCR QFF Quartic Force Constants^a (in mdyne/Åⁿ·rad^m).^b

F ₁₁₁₁	504.20	F ₇₇₁₁	0.47	F ₉₉₂₂	-0.10
F ₂₁₁₁	0.02	F ₇₇₂₁	0.00	F ₉₉₃₃	0.56
F ₂₂₁₁	0.34	F ₇₇₂₂	-0.02	F ₉₉₄₃	0.51
F ₂₂₂₁	1.79	F ₇₇₃₃	0.52	F ₉₉₄₄	0.40
F ₂₂₂₂	53.61	F ₇₇₄₃	0.58	F ₉₉₅₅	0.26
F ₃₃₁₁	504.15	F ₇₇₄₄	0.37	F ₉₉₆₅	0.02
F ₃₃₂₁	-0.15	F ₇₇₅₅	0.39	F ₉₉₆₆	0.27
F ₃₃₂₂	0.11	F ₇₇₆₅	-0.01	F ₉₉₇₇	0.37
F ₃₃₃₃	504.36	F ₇₇₆₆	0.33	F ₉₉₈₇	0.00
F ₄₃₁₁	-0.18	F ₇₇₇₇	0.31	F ₉₉₈₈	0.38
F ₄₃₂₁	-0.16	F ₈₇₁₁	-0.03	F ₉₉₉₉	0.36
F ₄₃₂₂	-0.48	F ₈₇₂₁	-0.12	F _{X731}	-26.98
F ₄₃₃₃	-0.21	F ₈₇₂₂	-0.40	F _{X732}	12.54
F ₄₄₁₁	0.38	F ₈₇₃₃	0.03	F _{X741}	-15.49
F ₄₄₂₁	-0.31	F ₈₇₄₃	-0.03	F _{X742}	7.56
F ₄₄₂₂	22.18	F ₈₇₄₄	0.07	F _{X831}	5.12
F ₄₄₃₃	0.45	F ₈₇₅₅	-0.01	F _{X832}	-2.45
F ₄₄₄₃	-0.15	F ₈₇₆₅	-0.08	F _{X841}	3.23
F ₄₄₄₄	35.67	F ₈₇₆₆	-0.06	F _{X842}	-1.59
F ₅₅₁₁	0.47	F ₈₇₇₇	0.03	F _{X931}	0.00
F ₅₅₂₁	0.00	F ₈₈₁₁	0.37	F _{X932}	0.00
F ₅₅₂₂	-0.01	F ₈₈₂₁	0.12	F _{X941}	0.01
F ₅₅₃₃	0.54	F ₈₈₂₂	1.83	F _{X942}	0.00
F ₅₅₄₃	0.58	F ₈₈₃₃	0.37	F _{X975}	0.05
F ₅₅₄₄	0.39	F ₈₈₄₃	-0.06	F _{X976}	-0.04
F ₅₅₅₅	0.34	F ₈₈₄₄	-0.53	F _{X985}	-0.04
F ₆₅₁₁	-0.03	F ₈₈₅₅	0.34	F _{X986}	-0.11
F ₆₅₂₁	-0.10	F ₈₈₆₅	-0.09	F _{XX11}	0.41
F ₆₅₂₂	-0.40	F ₈₈₆₆	0.83	F _{XX21}	-0.08
F ₆₅₃₃	0.05	F ₈₈₇₇	0.27	F _{XX22}	-0.10
F ₆₅₄₃	-0.04	F ₈₈₈₇	-0.15	F _{XX33}	0.53
F ₆₅₄₄	0.07	F ₈₈₈₈	1.16	F _{XX43}	0.49
F ₆₅₅₅	0.04	F ₉₅₃₁	0.18	F _{XX44}	0.39
F ₆₆₁₁	0.37	F ₉₅₃₂	0.03	F _{XX55}	0.37
F ₆₆₂₁	0.12	F ₉₅₄₁	0.55	F _{XX65}	-0.01
F ₆₆₂₂	1.83	F ₉₅₄₂	0.16	F _{XX66}	0.36
F ₆₆₃₃	0.37	F ₉₆₃₁	0.05	F _{XX77}	0.23
F ₆₆₄₃	-0.07	F ₉₆₃₂	-0.11	F _{XX87}	0.02
F ₆₆₄₄	-0.54	F ₉₆₄₁	-0.04	F _{XX88}	0.26
F ₆₆₅₅	0.31	F ₉₆₄₂	-0.06	F _{XX99}	0.37
F ₆₆₆₅	-0.14	F ₉₉₁₁	0.42	F _{XXXX}	0.37
F ₆₆₆₆	1.15	F ₉₉₂₁	-0.07		

^aSame note as ^a in Table 2. ^bThe units are the in same fashion as Table 2.

Table 4: Geometry and energy comparison of the global minimum between the results of the PES and the indicated *ab initio*(CCSD(T)-F12b/aug-cc-pVTZ) calculation.

	PES	<i>ab initio</i>
R ₁ (N-N)	1.097006Å	1.097001Å
R ₂ (N-N)	1.097006Å	1.097001Å
R ₁ (N-H)	1.276604Å	1.276677Å
R ₂ (N-H)	1.276604Å	1.276677Å
Energy(hatree)	-219.03515569	-219.03515567

Table 5: Comparison of harmonic frequencies(cm^{-1}) at the global minimum between the results of the PES and the indicated *ab initio*(CCSD(T)-F12b/aug-cc-pVTZ) calculation.

Mode	PES	<i>ab initio</i>
1	93.0	89.7
2	141.3	141.4
3	141.3	141.4
4	265.1	265.1
5	436.4	437.6
6	1223.0	1230.6
7	1223.0	1230.6
8	2384.6	2384.5
9	2420.6	2420.4

Table 6: The NNHNN⁺ CCSD(T)-F12/aug-cc-pVTZ-F12b PES harmonic frequencies at the global minimum structure, MULTIMODE VSCF/VCI zero point and energies for 5MR, 6MR cases, Diffusion Monte Carlo zero point and proton transfer fundamental (in cm^{-1}). MP2/aug-cc-pVTZ double harmonic Intensities and MULTIMODE intensities (in parentheses in km/mol).

	Harmonic	5MR	6MR	Other	Experiment ¹³
$\nu_1 \sigma_g$ N–N symm. stretch	2420.6	2335 ^m ,2376 ^m	2335 ^m ,2380 ^m	2396.4 ^a	2228 ^d
$\nu_2 \sigma_u$ N–N antisymm. stretch	2384.4(241)	2355.79(213.9)	2355.83	2363.9 ^a	2350
$\nu_3 \sigma_g$ N–H symm. stretch	436.4	385.6	385.4	432.5 ^a	381 ^d
$\nu_4 \pi_u \perp$ proton motion	1223.0(86)	1165.8(68.2)	1165.3	1302.3 ^a	1144
$\nu_5 \pi_g$ N–N–H symm. bend	265.1	260.4	260.2	263.8 ^a	240 ^d
$\nu_6 \pi_u$ N–N–H antisymm. bend	141.3(7)	146.0(8.5)	146.3	148.7 ^a	154 ^d
$\nu_7 \sigma_u$ N–H antisymm. stretch	93.0(5170)	758.84(2928.9)	757.40	1227.2 ^b / 746.3 ^c	743
$2\nu_3$	–	780.3	783.5	–	780
$\nu_4+\nu_6$	–	1329.5	1328.6	–	1300
$\nu_5+\nu_7$	–	1014.1(21.1)	1009.2	–	983
$\nu_3+\nu_4$	–	1510.2	1508.4	–	1409
Zero-Point Energy	4296.6	4571.0	4570.8	4561.9 ^c	–

^aVPT2 results, ^b1-D-DVR result, ^cDMC results, ^mmixed (see text), ^dnot directly measured